COMPRESSIBLE LAMINAR BOUNDARY LAYER ON A DELTA WING WITH ATTACHED SHOCK WAVE

V. N. Vetlutskii and T. V. Poplavskaya

UDC 532.526

1. In supersonic flow past a delta wing the flow behind the shock wave can be split into the inviscid region and the boundary layer if the Reynolds number is sufficiently large. The flow conditions around a delta wind at an angle of attack are shown in Fig. 1 [1-5] (on a sphere with center at the vertex of the plate). The classification is made according to the nature of the flow in the neighborhood of the leading edges (conditions A and B) as well as according to the presence and location of stagnation streamlines at the plate surface (conditions 1-3).

A corresponds to a supersonic leading edge, while B is subsonic. In this case the leading-edge shock is attached to the vertex of the wing and the inviscid flow is conical. There is also another case when the leading-edge shock moves away from the vertex and the flow becomes significantly three dimensional. However, we shall restrict our discussions to only conical flows.

Thd dividing streamline surface approaches the leading edge under conditions 1, whether the leading edges are supersonic or subsonic. The transverse velocity component is away from the leading edges in the plane of symmetry where the windward and leeward sides of the wing are located along one streamline. With an increase in angle of attack the conical dividing stream surface rotates towards the plane of symmetry. Starting from a certain moment when it approaches the wind orthogonally, further increase in the angle of attack leads to its displacement in the direction of the plane of symmetry (condition 2), while the approach angle to the wing, as shown in [6], remains normal. In this case there are two separation streamlines located on the surface of the wing. Starting from a certain angle of attack the separation streamlines merge with the stagnation streamline, and then the case 3 is realized with one separation streamline from the windward side.

Strictly speaking, conical flow under the above conditions can occur only when the influence of the trailing edge does not propagate upstream. This can be realized when the velocity component along the conical surface is supersonic. Otherwise the conical flow can be considered only as an approximation in the neighborhood of the vertex. It has been shown [7] that for thin slender wings the condition 3 in the above sense can be realized up to an angle of attack of the order of 90°, when the flow from the windward side along the conical surface is directed towards the vertex.

If the angle between the wing leading edge and the plane of symmetry is greater than the free-stream Mach angle, then with an increase in the angle of attack from zero to the limiting case the wing undergoes all conditions shown in Fig. 1. Otherwise, all flow situations except A1 are realized.

Inviscid flow past a delta wing under flow condition A1 was studied in [8], where detailed tables of the flow field from the windward and leeward sides are given for a wide range of Mach numbers and sweep. In [3, 5, 9] computations have been carried out for conical flow past a wing and cambered wings under conditions B1 and B2. In order to compute the boundary layer on the wing it is necessary to know the pressure distribution at its outer boundary, one velocity component (preferably the transverse component), and the value of entropy function. Unfortunately, it is not possible to use the results in these papers to compute the boundary layer. The inviscid flow field past a delta wing for condition B3 are obtained in [10, 11].

In the case of conical flow, three-dimensional boundary-layer equations allow similarity solution with two independent variables, one of which is the normal based on the square root of the distance along the generatrix [12]. In similarity variables, the boundary layer may

Novosibirsk. Translated from Zhurnal Prikladnoi Mekhaniki i Tekhnicheskoi Fiziki, No. 5, pp. 23-29, September-October, 1985. Original article submitted July 12, 1984.

 0021-8944/85/2605-0624$09.50

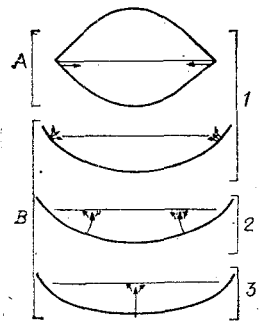

Fig. 1

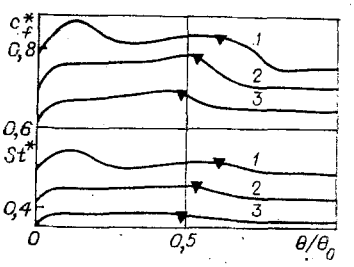

Fig. 2

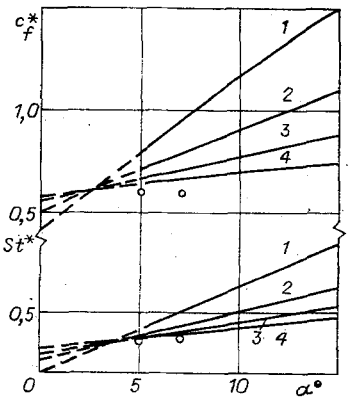

Fig. 3

be computed using a marching technique in the direction of velocity components normal to the generatrix. This means that under condition 3 the computation should start from the plane of symmetry.

The laminar boundary layer on the windward side of a delta wing was first studied in [4], where the method of integral relations was used to compute the flow under conditions 3. The initial conditions in the plane of symmetry were obtained from the solution of the very equations written in this plane. The outer boundary conditions for the boundary layer were taken from [10].

In the case 2, boundary-layer equations in similarity variables on the windward side should be solved from separating streamlines on both sides. Similar flow conditions were considered for an elliptic cone at small angles of attack [13, 14].

In [15-17] hypersonic boundary layers on delta wings were considered. The inverse effect of the boundary layer on the inviscid flow was studied using the pressure distribution computed from "tangential wedge" equations. Solutions have been obtained for boundary-layer equations with weak and strong interactions. Results show that reverse flow in the transverse direction could arise in the flow past delta wing under the given conditions, i.e., there is a transverse boundary-layer separation [16].

The present paper discusses a similar laminar boundary layer on the windward side of a delta wing under conditions A1. From the point of view of the boundary layer, there is no difference between the nature of flow under conditions A1 and B1. In both cases the velocity component normal to the generatrix at the outer edge of the boundary layer is directed from the leading edges towards the plane of symmetry.

2. The laminar boundary layer on a flat delta wing with a leading edge sweep χ is considered. The free-stream velocity vector U_∞ lies in the plane of symmetry of the wing and is at an angle of attack α to its surface. A cylindrical coordinate system (r, θ, z) is used, where r is the distance from the vertex of the wing along its surface, θ is the angle measured from the plane of symmetry, and z is the distance along the normal to the wing.

Compressible boundary-layer equations for delta wing are taken from [18]. These equations allow a similarity solution in two variables θ and $\eta = z/\sqrt{r}$ [12, 6] with conical outer flow and isothermal wing or in the case of an insulated wall; r and z are nondimensionalized with respect to certain reference length. The system of equations in these variables is given in [6]. It is evolutionary and can be solved using a marching technique along the variable θ, with the marching direction coinciding with the direction of the transverse velocity component v. In the present flow condition A1 the flow is from the leading edges to the plane of symmetry, and therefore, initial conditions are specified near the leading edges.

Similarity variables $\omega = \theta_0 - \theta$, $\eta = z/\sqrt{r(\theta_0 - \theta)}$ are introduced, where θ_0 is leading edge angle of the wing ($\theta_0 = 90 - \chi$). In the neighborhood of the leading edge the variable η is like the Blasius variable and hence the boundary-layer equations in these variables do not have singularity at the leading edge. In order to reduce the gradients of all the desired functions in η, a logarithmic stretching has been carried out [12, 6]

$$\xi = f(\eta/L) = \ln(1 + \eta/\varepsilon_2 L)/\ln(1 + 1/\varepsilon_2),$$

where $L = L(\omega)$ is the scaled boundary layer thickness and ε_2 is the stretching parameter.

Thus the system of laminar boundary layer equations in variables ω, ξ has the form

$$\frac{f'}{L}\frac{\partial J}{\partial \xi}+\omega\left(\frac{3}{2}\rho u-\frac{\partial \rho v}{\partial \omega}\right)-\frac{1}{2}\rho v-\frac{f'}{L}\omega\frac{L'}{L}\rho v N=0,$$

$$J\frac{f'}{L}\frac{\partial u}{\partial \xi}-\omega\rho v\left(\frac{\partial u}{\partial \omega}+v\right)-\frac{f'}{L}\frac{\partial}{\partial \xi}\left(\mu\frac{f'}{L}\frac{\partial u}{\partial \xi}\right)=-\omega\rho_e v_e\left(\frac{\partial u_e}{\partial \omega}+v_e\right),$$

$$J\frac{f'}{L}\frac{\partial v}{\partial \xi}+\omega\rho v\left(u-\frac{\partial v}{\partial \omega}\right)-\frac{f'}{L}\frac{\partial}{\partial \xi}\left(\mu\frac{f'}{L}\frac{\partial v}{\partial \xi}\right)=\omega\rho_e v_e\left(u_e-\frac{\partial v_e}{\partial \omega}\right), \tag{2.1}$$

$$c_p J\frac{f'}{L}\frac{\partial T}{\partial \xi}-\omega c_p\rho v\frac{\partial T}{\partial \omega}-\frac{1}{\mathrm{Pr}}\frac{f'}{L}\frac{\partial}{\partial \xi}\left(k\frac{f'}{L}\frac{\partial T}{\partial \xi}\right)=-\omega c_{p_e}\rho_e v\frac{\partial T_e}{\partial \omega}+\mathrm{M}_\infty^2(\gamma-1)\mu\left(\frac{f'}{L}\right)^2\left[\left(\frac{\partial u}{\partial \xi}\right)^2+\left(\frac{\partial v}{\partial \xi}\right)^2\right],$$

$$p=\frac{1}{\gamma \mathrm{M}_\infty^2}\rho T.$$

The problem was solved with the following boundary conditions:

$$\begin{aligned}&\omega=0:\ u=u_0(\xi),\ v=v_0(\xi),\ T=T_0(\xi),\\&\xi=0:\ u=v=J=0,\ T=T_w,\\&\xi=1:\ u=u_e(\omega),\ v=v_e(\omega),\ T=T_e(\omega),\ p=p_e(\omega).\end{aligned} \tag{2.2}$$

Here mass flow J and function $N(\omega, \xi)$ have been introduced:

$$J=\rho\sqrt{\omega}\left(-0.5\eta u+\sqrt{\omega}\frac{L'}{L}\eta v+w\sqrt{r}\right)+0.5\rho\eta v,$$

$$N=\frac{\partial \eta}{\partial \xi}=L(\omega)\varepsilon_2\exp(\xi\ln(1+1/\varepsilon_2))\ln(1+1/\varepsilon_2).$$

Primes denote differentiation of functions with respect to their own argument. Velocity components u and v are nondimensionalized with respect to the free stream velocity U_∞, pressure p is with respect to twice the dynamic pressure $\rho_\infty U_\infty^2$, dynamic viscosity μ, heat conductivity k, specific heat at constant pressure c_p, density ρ, and temperature T are nondimensionalized with respect to their free-stream values.

Initial profiles $u_0(\xi)$, $v_0(\xi)$, and $T_0(\xi)$ were determined from the solution of ordinary differential equations obtained from Eqs. (2.1) as $\omega \to 0$ with the assumption that all functions and their derivatives are bounded [19]. Pressure distribution p_e and transverse velocity components were specified in Cartesian coordinates at the outer edge of the boundary layer from the computations of the inviscid flow [8]. The parameters u_e, v_e, and T_e were computed using these data and also Bernoulli's equation and entropy.

3. Equations of motion and energy from (2.1) may be written in the general form

$$a\frac{\partial f}{\partial \omega}+b\frac{\partial f}{\partial \xi}+e\frac{\partial}{\partial \xi}\left(c\frac{\partial f}{\partial \xi}\right)+d=0, \tag{3.1}$$

where f denotes u, v, or T. In order to solve equations of the type (3.1), a two-layer, implicit scheme with weighting [20] was used. Viscosity and heat conductivity were approximated by the power law $\mu=T^{0.76}$. The nonlinearity of the system (3.1) requires an iterational approach which makes it possible to bring the problem within one iteration to scalar shooting method for difference boundary-value problems, approximating the equations of motion and energy. The coefficients and arbitrary terms in (3.1) at each iteration were computed from the values of parameters obtained in the previous iteration. Mass flow rate J was determined from the continuity equation. Iterations were continued until the functions at each point converged within specified accuracy.

Initial profiles $u_0(\xi)$, $v_0(\xi)$, $T_0(\xi)$ were obtained from the solution of ordinary differential equations at $\omega = 0$, written in difference form. Subsequently the two-dimensional difference equations were solved up to the plane of symmetry [19].

Velocity and temperature profiles in the boundary layer on the windward side of the wing were obtained as a result of the solution of the problem (2.1) and (2.2). They are used to compute the local skin-friction coefficients in the streamwise c_{f1} and transverse c_{f2} directions, local heat transfer coefficient St (Stanton number), and the absolute value of the resultant local skin-friction coefficient c_f:

$$c_{f1}=\mu\frac{\partial u}{\partial z}\Big|_{z=0}\Big/0{,}5\rho_\infty U_\infty^2,\quad c_{f2}=\mu\frac{\partial v}{\partial z}\Big|_{z=0}\Big/0{.}5\rho_\infty U_\infty^2,$$

$$c_f = \sqrt{c_{f1}^2 + c_{f2}^2}, \quad \mathrm{St} = k\frac{\partial T}{\partial z}\Big|_{z=0} \Big/ \rho_\infty U_\infty (h_\infty - h_w), \tag{3.2}$$

where h is the total enthalpy of the flow.

For the ease of computation and graphical representation, local similarity parameters depending only on the variable ω were used:

$$c_{f1}^* = c_{f1}\sqrt{\mathrm{Re}_r\omega}, \quad c_{f2}^* = c_{f2}\sqrt{\mathrm{Re}_r\omega}, \quad c_f^* = c_f\sqrt{\mathrm{Re}_r\omega}, \quad \mathrm{St}^* = \mathrm{St}\sqrt{\mathrm{Re}_r\omega},$$

where Re_r is the local Reynolds number based on free-stream parameters and the distance r from the wing vertex.

4. Computations of laminar boundary-layer parameters on the windward side of the delta wing were carried out for all variants given in [8] with supersonic leading edges. The range in variation of sweep was 45-75°, in angle of attack 5-15°, and in Mach number 2-10. Computed results for the flow fields, with the ratio of well enthalpy to free-stream enthalpy $H_w = 0.1$, are given in the form of a tables in [21]. In all the cases the number of steps along the coordinate ω was 80 and along ξ, 50. It should be mentioned that there was no transverse separation of the boundary layer.

As an example, the variation of local similarity coefficients of skin friction c_f^* and St* is shown in Fig. 2 as a function of the angle θ with $\chi = 45°$, $M_\infty = 3.0$, $H_w = 0.1$, and $\alpha = 15$, 10, and 5° (curves 1-3, respectively). The nature of these curves significantly differs from that given in [4] for the condition B3. In the case A1 the inviscid flow past the leading edge is similar to the flow past a tapered wedge [1]. Hence in the neighborhood of the leading edge, the flow parameters outside the boundary layer are constant right up to the Mach cone of the disturbed flow along which the uniform flow becomes conical. In the uniform external flow the parameters c_f^* and St* are constant, and during the transition through the Mach cone their values increase. The Mach cone is traced by the curve with triangles. A sharp decrease in c_f^* and St* near the plane of symmetry was discussed in [19].

With an increase in the angle of attack, the nature of curves c_f^* and St* changes slowly and the transition zone from constant values is somewhat displaced. It is possible to say that the dependence on the angle of attack is practically linear. This is observed well in Fig. 3, where the values of c_f^* and St* near the leading edge are shown as a function of angle of attack with $\chi = 45°$, $H_w = 0.1$, and $M_\infty = 10$, 6, 4, and 3 (curves 1-4), circles indicate values of c_f^* and St* corresponding to $M_\infty = 2$, and dashes indicate extrapolated curves. The practically linear dependence on angle of attack and free-stream Mach number is clearly seen. Hence c_f^* and St* may be approximately described by the following interpolation equations near the leading edges with $\chi = 45°$ and $H_w = 0.1$:

$$\begin{aligned} c_f^* &= 0.61 + (0.0089\,M_\infty - 0.015)(\alpha - 2.6), \\ \mathrm{St}^* &= 0.34 + (0.0043\,M_\infty - 0.0004)(\alpha - 3.4), \end{aligned} \tag{4.1}$$

where the angle of attack is given in degrees. Here the error in c_f^* does not exceed 1.5% and for St* – 2% in the range of Mach numbers 3-10 and angles of attack 5-15°.

As expected, the region of uniform flow increases with Mach number with the reduction in Mach angle of the disturbed flow. Consequently, the region with constant c_f^* and St* also increases.

Computations were carried out for the boundary layer at zero angle of attack. The parameters c_i^* and St* in this case depend on ω as $(\omega/\sin\omega)^{1/2}$ which agrees well with the results obtained. Table 1 gives values of c_f^* and St* near the leading edge with $\chi = 45°$, $H_w = 0.1$, and $M_\infty = 2$, 3, 4, 6, and 10. Interpolation Eqs. (4.1) at $\alpha = 0$ give values of c_f^* at $M_\infty = 3$-6 within the specified error and when $M_\infty = 10$, lower it by 10%. The value of St* is lowered by the interpolation equation by 4-6% at $M_\infty = 3$-6 and by 19% at $M_\infty = 10$.

An increase in M_∞ leads to a thickening of the boundary layer and hence the values of c_f^* and St* decrease somewhat for the isothermal wall. Since the computations were carried out for a constant ratio of wall enthalpy H_w, these parameters are multiplied by the factor $(1 + (\gamma - 1)M_\infty^2/2)^d$, where $d = 0.76$ is the exponent in the relation between viscosity and temperature. All together lead to a practically linear dependence of c_f^* and St* on M_∞ for $\alpha \geqslant 5°$. Similar influence of M_∞ was observed at high angles of attack [4]. However, with a decrease in angle of attack the dependence of boundary-layer thickness on M_∞ rapidly increases and the associated significant decrease in the velocity gradient along the normal results in inverse dependence of c_f^* and St* on M_∞ at $\alpha = 0$.

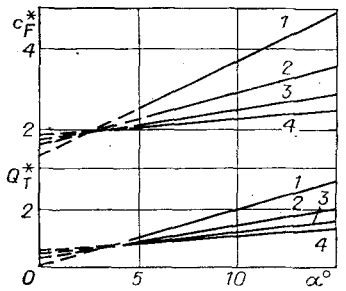

Fig. 4

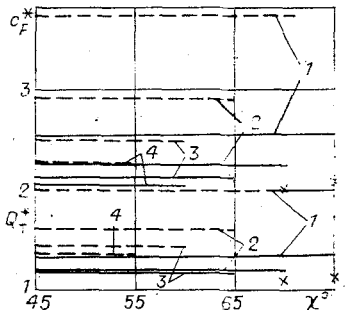

Fig. 5

TABLE 1

M_∞	2	3	4	6	10
c_f^*	0,588	0,567	0,548	0,513	0,465
St*	0,336	0,312	0,295	0,270	0,241
c_F^*	1,869	1,803	1,740	1,631	1,479
Q_T^*	1,068	0,992	0,936	0,857	0,765

The values of c_f^* and St* decrease with an increase in sweep χ. A change in relative enthalpy of the wing surface H_w has relatively small effect on them. Thus an increase in H_w from 0.05 to 0.1 resulted in a decrease in c_f^* by not more than 1.5% and St* by 2.5%, and when H_w is increased by an order of magnitude c_f^* changed by not more than 7% and St* by 20%.

In addition to local parameters, the integral similarity coefficients of skin friction c_F^* and heat flux Q_T^* along the windward side of the wing were also computed:

$$c_F^* = c_F\sqrt{\mathrm{Re}_L} = \frac{X\sqrt{\mathrm{Re}_L}}{0{,}5\rho_\infty U_\infty^2 S} = \frac{4}{3\,\mathrm{tg}\,\theta_0}\int_0^{\theta_0}\frac{c_f^*\cos\vartheta}{\sqrt{\omega\cos(\theta_0-\omega)}\cos(\theta_0-\omega)}\,d\omega,$$

$$Q_T^* = Q_T\sqrt{\mathrm{Re}_L} = \frac{Q\sqrt{\mathrm{Re}_L}}{\rho_\infty U_\infty(h_\infty - h_w)S} = \frac{4}{3\,\mathrm{tg}\,\theta_0}\int_0^{\theta_0}\frac{\mathrm{St}^*}{\sqrt{\omega\cos(\theta_0-\omega)}\cos(\theta_0-\omega)}\,d\omega,$$

where X and Q are skin friction and heat flux to the windward side of the wing; L is the length of the central chord; S is the wing area; ϑ is the angle of inclination of the local shear stress coefficient to the plane of symmetry:

$$\vartheta = \mathrm{arctg}\,(c_{f2}^*/c_{f1}^*) + \theta_0 - \omega.$$

Figure 4 shows parameters c_F^* and Q_T^* as functions of angle of attack with $\chi = 45°$, $H_w = 0.1$, and different values of M_∞; the numbering of curves is according to Fig. 3, circles denote data for $M_\infty = 2$. The behavior of c_F^* and Q_T^* resembles the behavior of c_f^* and St* near the leading edge. Interpolation functions for $\chi = 45°$ and $H_w = 0.1$ have also been obtained:

$$c_F^* = 1.96 + (0{,}029\,M_\infty - 0.044)(\alpha - 2.9), \quad Q_T^* = 1.13 + (0.015\,M_\infty - 0.006)(\alpha - 4), \qquad (4.2)$$

where the angle of attack α is given in degrees. The error in these equations for c_F^* and Q_T^* does not exceed 1% in the range M_∞ = 3-6 and angles of attack 5-15°. For $M_\infty = 10$ this error increases to 2 and 4%, respectively.

Table 1 also gives computed results for the same variations with $\alpha = 0$. Interpolated values of c_F^* (4.2) differ from exact by 2-3% at M_∞ = 3-6 and happen to be lower by 15.5% at $M_\infty = 10$. For the parameter Q_T the interpolation formula (4.2) gives lower results by 1.5, 3, 8, and 25.5% for M_∞ = 3, 4, 6, and 10, respectively.

The dependence of parameters c_F^* and Q_T^* on the sweep angle at $H_w = 0.1$ and different Mach numbers is shown in Fig. 5, with numbering corresponding to Fig. 3, continuous lines for

$\alpha = 5°$, dashed lines for $\alpha = 10°$; the curves 3 and 4 at $\alpha = 5°$ merge together. Results from [4] are indicated by crosses for comparison for $M_\infty = 6$, $\alpha = 5°$, $H_w = 0.05$, and the difference at $\chi = 70$ is about 10%. It is seen that parameters c_F^* and Q_T^* do not depend on sweep except at $M = 10$ where the deviation does not exceed 2-3%. This means that the interpolation functions (4.2) may be used in the range of sweep angles 45-75° and $M_\infty = 3$-6, with an accuracy of 1.5% for c_F^* and 2% for Q_T^*. When $M_\infty = 10$ this error increases to 5 and 7%, respectively.

The influence of wall enthalpy H_w on boundary-layer parameters was explained by the following variant: $\chi = 70°$, $M_\infty = 6$, and $\alpha = 5°$. Computations showed that in changing H_w from 0.05 to 0.1 the value of c_F^* decreases by 1% and Q_T^* by 3%. However, an increase in H_w by an order of magnitude leads to their decrease by 5 and 19%, respectively.

LITERATURE CITED

1. B. M. Bulakh, Nonlinear Conical Flow of Gases [in Russian], Nauka, Moscow (1970).
2. G. G. Chernyi, "Wings in hypersonic flow," Prikl. Mat. Mekh., 29, No. 4 (1965).
3. A. P. Bazzhin and I. F. Chelysheva, "Numerical solution to supersonic flow past plane delta wing at small angles of attack," Uchen. Zap. Tsentral'nyi Aerogidrodinamicheskii Institut (TsAGI), 5, No. 5 (1974).
4. V. A. Bashkin, "Compressible laminar boundary layer in conical external flow," Tr. TsAGI, 1093 (1968).
5. A. N. Minailos, "Supersonic flow past thin wings," Uchen. Zap. TsAGI, 8, No. 4 (1977).
6. V. N. Vetlutsky and V. L. Ganimedov, "Numerical solution of boundary layer on an elliptic cone," Chislen. Metody Mekh. Splosh. Sred., 8, No. 5 (1977).
7. G. G. Chernyi, "Hypersonic flow past wings at high angles of attack," Dokl. Akad. Nauk SSSR, 155, No. 2 (1964).
8. G. P. Voskresensky, A. S. Il'ina, and V. S. Tatarenchik, "Supersonic flow past wings with attached shock waves," Tr. TsAGI, 1590 (1974).
9. A. P. Kosikh, "Some results of numerical study on supersonic flow past finite-thickness delta wings," Tr. TsAGI, 1971 (1978).
10. A. P. Bazzhin, "Computation of perfect fluid flow past plane delta wings at high angles of attack," Tr. TsAGI, 1034 (1966).
11. A. P. Bazzhin, "Computation of flow on the lower surface of delta wings at large angles of attack," Inzh. Zh., 4, Issue 2 (1964).
12. N. D. Vvedenskaya, "Computation of boundary layer on a conical body at an angle of attack," Zh. Vychisl. Mat. Mat. Fiz., 6, No. 2 (1966).
13. V. N. Vetlutsky and V. L. Ganimedov, "Computation of laminar boundary layer on a sharp elliptic cone," in: Numerical Analysis [in Russian], Inst. Teor. Prikl. Mekh. Sib. Otd. Akad. Nauk SSSR, Novosibirsk (1978).
14. V. N. Velutsky and V. L. Ganimedov, "The investigation of a compressible laminar boundary layer past an elliptic cone," Comput. Fluids, 10, No. 3 (1982).
15. G. N. Dudin, "Interaction of hypersonic flow with boundary layer on a thin delta wing," Tr. TsAGI, 1912 (1978).
16. G. N. Dudin, "Computation of boundary layer on a delta wing with strong viscous interaction," Uchen. Zap. TsAGI, 9, No. 5 (1978).
17. G. N. Dudin and D. O. Lyzhin, "A method to compute strong viscous interaction on a delta wing," Izv. Akad. Nauk SSSR, Mekh. Zhidk. Gaza, No. 4 (1983).
18. Yu. D. Shevelev, Three-Dimensional Laminar Boundary Layer Theory [in Russian], Nauka, Moscow (1977).
19. V. N. Vetlutsky and T. V. Poplavskaya, "Computation of laminar boundary layer on a plane delta wing with supersonic leading edges," Chislen. Metody Mekh. Splosh. Sred., 13, No. 1 (1982).
20. Yu. I. Brailovskaya and L. A. Chudov, "Solution of boundary layer equations using finite-difference methods," in: Computational Methods and Programming [in Russian], Vol. 1, Vychislitel'nyi Tsentr, Mosk. Gos. Univ., Moscow (1962).
21. V. N. Vetlutsky and T. V. Poplavskaya, Tables of Laminar Boundary-Layer Parameters on the Windward Side of Delta Wing with Attached Leading-Edge Shock Wave [in Russian], Preprint No. 7-84, Inst. Teor. Prikl. Mekh., Sib. Otd. Akad. Nauk SSSR, Novosibirsk (1984).